DOI: https://doi.org/10.62985/j.huit_ojs.vol26.no2E.384

DESIGN AND OPTIMIZATION OF A 7.7 GHZ RF POWER AMPLIFIER USING GAN HEMT TRANSISTOR ON ROGERS 5880LZ SUBSTRATE

Hoai Nam Tran*, Manh Dan Do, Xuan Quynh Le, Van Tu Dinh

Faculty of Engineering Fundamentals, Naval Academy

30 Tran Phu Street, Nha Trang, Khanh Hoa, Vietnam

*Email: *Namphongtute@gmail.com*

Received: 11 January 2026; Revised: 5 March 2026; Accepted: 15 April 2026

ABSTRACT

This paper presents the design and simulation of a radio-frequency (RF) power amplifier operating at a center frequency of 7.7 GHz using a GaN HEMT transistor NP2500MS manufactured by Win Semiconductor on a Rogers 5880LZ substrate. The amplifier operates in Class-AB mode and employs input and output matching networks. To ensure unconditional stability, a 9.1 Ω resistor connected in series with the gate and paralleled with a 0.5-pF capacitor is introduced. Simulation results obtained using Keysight Advanced Design System (ADS) demonstrate that the proposed amplifier satisfies the design requirements, achieving S11 < −10 dB, S22 < −7.88 dB, S21 = 16.55 dB, a bandwidth of 6.9%, a maximum output power of 17.59 dBm, and DC power consumption below 0.3 W.

Keywords: RF power amplifier, GaN HEMT, Rogers 5880LZ, impedance matching, unconditional stability.

1. INTRODUCTION

RF power amplifiers (PAs) play a critical role in microwave and millimeter-wave communication systems, including radar, satellite communications, and wireless backhaul links. In C-band applications, power amplifiers are required to provide sufficient output power, high gain, wide bandwidth, and stable operation while maintaining low DC power consumption. These requirements become more challenging as operating frequencies increase, particularly when compact size and high efficiency are simultaneously desired.

For high-frequency microwave applications, GaN HEMT technology has emerged as a dominant alternative for power amplifier designs. This preference is primarily owing to its high breakdown voltage, substantial power density, and superior thermal properties compared to conventional GaAs and silicon-based technologies [3]. Consequently, GaN HEMT-based power amplifiers have been widely investigated for C-band and X-band applications [6, 7]. However, achieving unconditional stability over a wide bandwidth while preserving high gain remains a significant design challenge, especially when operating at relatively low DC power consumption [10].

Several stabilization techniques have been reported in the literature, including resistive loading, feedback networks, and lossy matching structures [1, 2]. Although these approaches can improve stability, they often result in reduced gain or increased power dissipation [2]. Therefore, a careful trade-off between stability, gain, and power efficiency is required, particularly for low-power RF applications [8].

In this paper, a 7.7-GHz RF power amplifier based on a GaN HEMT transistor is presented. The amplifier is implemented on a Rogers 5880LZ substrate and operates in Class-

AB mode to balance linearity and power efficiency. Unconditional stability is achieved by introducing a compact RC stabilization network at the gate of the transistor, which significantly improves the stability factor without severely degrading the maximum available gain. Input and output impedance matching networks are designed to meet the specified reflection coefficient and gain requirements over the target frequency band.

2. DESIGN METHODOLOGY

2.1. Circuit Diagram Construction

The proposed RF power amplifier employs a single GaN HEMT transistor configured in a common-source topology. Input and output impedance matching networks are used to ensure maximum power transfer. The circuit is designed and simulated using Keysight ADS.

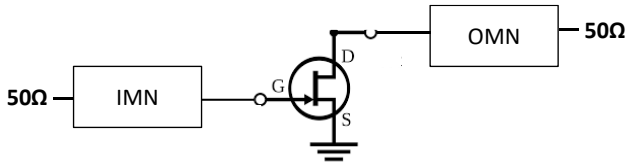

Fig. 1. Schematic of the proposed 7.7-GHz RF power amplifier.

2.2. Substrate Parameters

The amplifier is implemented on a Rogers 5880LZ substrate with the following parameters: relative permittivity εr = 2, loss tangent tanδ = 0.002, substrate thickness h = 0.252 mm, and copper thickness T = 35 μm [5].

Property	Typical Value [1] RT/duroid® 5880LZ	Direction
Dielectric Constant ε_r Process	2.00 ± 0.04	Z
[2] Dielectric Constant ε_r Design	2.00	Z
Dissipation Factor, tan	Typ: 0.0021 Max: 0.0027	Z

Standard Thicknesses
0.010" (0.252mm) +/- 0.0007"
0.020" (0.508mm) +/- 0.0015"
0.050" (1.270mm) +/- 0.0015"
*Additional non-standard thicknesses available 0.0075" and 0.010" - 0.200" in increments of 0.005"

Fig. 2. Rogers 5880LZ material parameters

2.3. DC Biasing and Operating Point

DC characteristics, transistor operating point

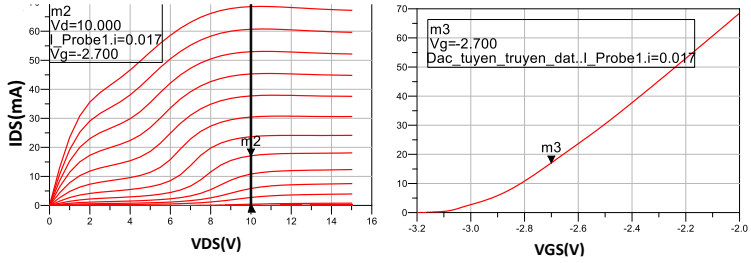

Fig. 3. Output characteristic and transfer characteristic

Based on the DC characteristics of the transistor, the operating point is selected at VDS = 10 V, VGS = −2.7 V, and IDS = 17 mA. Under this bias condition, the amplifier operates in Class-AB mode. The DC power consumption at the quiescent operating point is calculated as:

$$P_{DC} = V_{DS} \times I_{DS} = 10 \times 0.017 = 0.17 \text{ W}$$

2.4. Stability Analysis

S-Parameter Matrix of the GaN HEMT Transistor

At the 7.7-GHz operating frequency, the GaN HEMT device's scattering parameters are utilized to assess the proposed RF power amplifier's small-signal stability. These simulated matrix values are compiled in Table 1.

Table 1. Transistor Scattering Matrix Parameters

Freq	S(1,1)	S(1,2)	S(2,1)	S(2,2)
7.700 GHz	0.845 / -95.300	0.052 / 27.661	3.473 / 114.092	0.719 / -37.976

2.4.1. Source Stability Circle

The transistor's potential for stable operation is assessed by determining its source stability boundaries, which are derived via the subsequent formulations [1]. The S parameter matrix determinant was determined as follows

$$\Delta = S_{11}S_{22} - S_{12}S_{21} = \frac{0.619}{-116.365}$$

The center C_S and radius R_S of the source stability circle are calculated as

$$C_S = \frac{(S_{11} - \Delta S_{22}^*)^*}{|S11|^2 - |\Delta|^2} = 1.324/112.454$$

$$R_S = \left|\frac{S_{12}S_{21}}{|S_{11}|^2 - |\Delta|^2}\right| = 0.545$$

2.4.2. Load Stability Circle

Similarly, the center C_L and radius R_L of the load stability circle are calculated as

$$C_L = \frac{(S_{22} - \Delta S_{11}^*)^*}{|S_{22}|^2 - |\Delta|^2} = 1.987/72.831$$

$$R_L = \left|\frac{S_{12}S_{21}}{|S_{22}|^2 - |\Delta|^2}\right| = 1.348$$

The calculated source and load stability circles are plotted on the Smith chart, as shown in Fig. 4, to identify the stable and unstable regions.

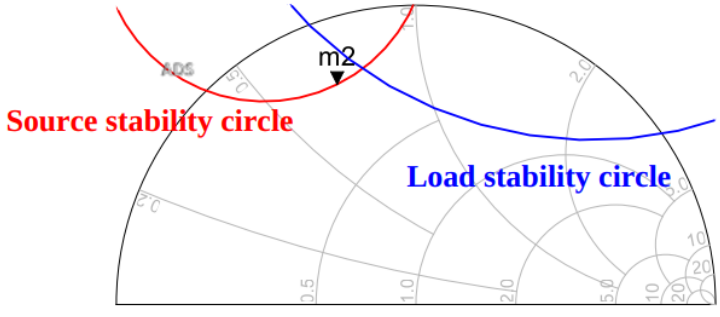

Fig. 4. Source and load stability circles plotted on the Smith chart.

2.4.3. Stability Factor

To further evaluate the stability condition of the transistor, the stability factor μ is calculated as [1].

$$\mu = \frac{1 - |S_{11}|^2}{|S_{22} - \Delta S_{11}^*| + |S_{12}S_{21}|} = 0.638 < 1$$

At the operating frequency of 7.7 GHz, the calculated value of the stability factor is

$$\mu = 0.638 < 1$$

which indicates that the GaN HEMT transistor is conditionally stable.

For a conditionally stable device, the source and load impedances Z_S and Z_L must be carefully selected to lie within the stable regions on the Smith chart, and preferably far from the unstable regions. However, in RF power amplifier design targeting high gain, the load impedance Z_L is often chosen primarily to maximize gain rather than to satisfy output matching conditions. As a result, the output reflection coefficient S_{22} may become relatively large, and in some cases even exceed 0 dB.

Therefore, to satisfy the design requirement of $S_{22} \leq -5$ dB over the operating bandwidth, the RF power amplifier must be designed to operate under unconditional stability. This motivates the introduction of an additional stabilization network, which is discussed in the following section.

2.4.4. Stabilization Using Series Gate Resistor

Integrating a resistive component in series with the drain or gate terminal represents an efficient method for ensuring unconditional stability in RF transistors. For the present design, a series gate resistor is selected owing to its practical simplicity and proven efficacy.

The input stability boundary dictates the required value for this series resistor. In particular, the resistance is established by locating where the source stability circle interfaces tangentially with the real axis of the Smith chart. As illustrated by marker m2 in Fig. 5, the real component of the impedance at this specific intersection is roughly 9.1 Ω.

Therefore, a resistor with a value of 9.1 Ω is connected in series with the gate of the GaN HEMT transistor.

Once the series gate resistor is integrated, the combined resistor-transistor structure is modeled as a unified two-port network to extract a fresh set of scattering parameters. These revised S-parameter values computed at 7.7 GHz are compiled in Table 2.

Table 2. S-parameters of the GaN HEMT transistor with series gate resistor.

Freq	S(1,1)	S(1,2)	S(2,1)	S(2,2)
7.700 GHz	0.695 / -92.490	0.047 / 23.671	3.155 / 110.103	0.704 / -37.885

2.4.5. Stability Verification and Maximum Gain Analysis

Following the integration of the series gate resistor, the device's stability performance undergoes a re-assessment. The resulting source and load stability boundaries for the stabilized transistor are projected onto the Smith chart, as illustrated in Fig. 5.

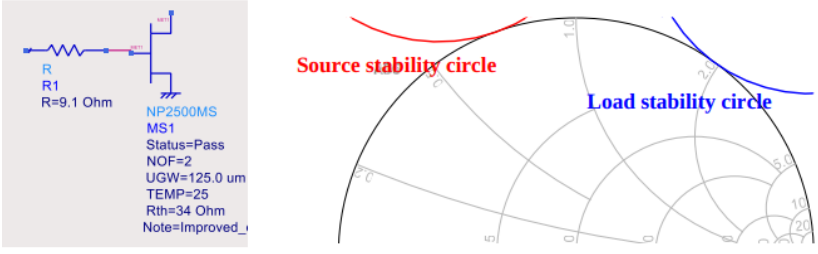

Fig. 5. Source and load stability circles of the transistor with series gate resistor.

To quantitatively assess the stability condition, the stability factor μ is recalculated using

$$\mu = \frac{1 - |S_{11}|^2}{|S_{22} - \Delta S_{11}^*| + |S_{12}S_{21}|} = 1$$

The calculated value of the stability factor is

$$\mu = 1$$

indicating that the GaN HEMT transistor becomes unconditionally stable after the addition of the series gate resistor.

2.4.6. Maximum Gain Analysis

For the original transistor, which exhibits conditional stability, the maximum stable gain (MSG) is given by

$$G_{MSG} = \left| \frac{S_{21}}{S_{12}} \right| = 18.24 \text{ dB}$$

After introducing the series gate resistor, the transistor operates under unconditional stability. Therefore, the maximum available gain (MAG) is calculated as

$$G_{MAG} = \left| \frac{S_{21}}{S_{12}} \right| \left(k - \sqrt{k^2 - 1}\right)$$

where the Rollet stability factor $k$is given by

$$k = \frac{1 - |S_{11}|^2 - |S_{22}|^2 + |\Delta|^2}{2\,|S_{12}S_{21}|}$$

For the stabilized transistor, the calculated value of $k$is approximately 0.997, resulting in

$$G_{MAG} = 18.241 \text{ dB}$$

This result indicates that the introduction of the series gate resistor does not significantly degrade the maximum achievable gain of the transistor at the target frequency of 7.7 GHz.

To further investigate the gain behavior over frequency, a parametric simulation is performed in Keysight ADS over the frequency range from 7.5 GHz to 7.9 GHz. The simulated maximum gain characteristics are shown in Fig. 6.

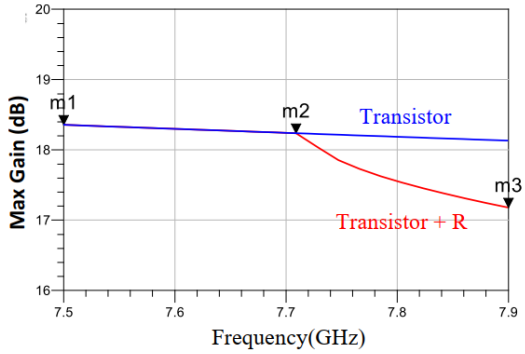

Fig. 6. Maximum gain of the transistor before and after adding the series gate resistor.

2.4.7. Gain Compensation Using Parallel Capacitor

As observed in the frequency range from 7.7 GHz to 7.9 GHz, the maximum gain of the transistor with only the series gate resistor decreases compared to the unstabilized case. This behavior occurs because, at frequencies above 7.7 GHz, the tangency point of the source

stability circle corresponds to a resistance value lower than 9.1 Ω. Consequently, the fixed 9.1 Ω series resistor introduces additional loss, leading to a reduction in the maximum achievable gain.

To mitigate this gain degradation, a shunt capacitor is added in parallel with the series gate resistor. The capacitor value is selected as 0.5 pF, forming an RC stabilization network connected in series with the gate of the GaN HEMT transistor. This RC network provides frequency-dependent compensation, effectively reducing the resistive loss at higher frequencies while preserving unconditional stability. A similar approach utilizing compact RC networks for stabilizing and preserving high-frequency available gain in Class-AB GaN HEMT power amplifiers operating across the C-band has been validated in [8] and [9].

The simulation results obtained after adding the parallel capacitor are shown in Fig. 7.

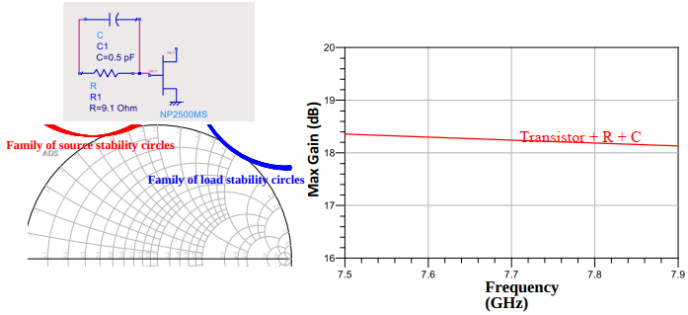

Fig. 7. Simulated performance after adding the series gate resistor and parallel capacitor.

After introducing the RC stabilization network, a new set of S-parameters is extracted by treating the RC network and the transistor as a single two-port network. The updated S parameter values at 7.7 GHz are summarized in Table 3.

Table 3. S-parameters of the transistor with RC stabilization network.

Freq	S(1,1)	S(1,2)	S(2,1)	S(2,2)
7.700 GHz	0.711 / -90.415	0.047 / 24.955	3.127 / 111.386	0.705 / -37.664

The simulation results confirm that the RC stabilization network effectively restores the maximum gain while maintaining unconditional stability. The maximum achievable gain reaches 18.24 dB, 18.35 dB, and 18.13 dB at 7.7 GHz, 7.5 GHz, and 7.9 GHz, respectively.

For practical implementation, commercially available surface-mount components are employed. The series resistor is a 9.1-Ω, 0603-size resistor manufactured by Panasonic, while the shunt capacitor is a 0603-size capacitor manufactured by Murata. These components ensure ease of fabrication and consistency between simulation and practical realization [6, 7].

2.4.8. Unilateral figure of merit (U-factor)

To assess whether the unilateral assumption is valid, the unilateral figure of merit $U$is evaluated as

$$U = \frac{|S_{12}||S_{21}||S_{11}||S_{22}|}{(1-|S_{11}|^2)(1-|S_{22}|^2)} = 0.295$$

The corresponding unilateral gain error bound is given by

$$\frac{1}{(1+U)^2} < \frac{G_T}{G_{TU}} < \frac{1}{(1-U)^2}$$

$$-2.248 = \frac{1}{(1+U)^2} < \frac{G_T}{G_{TU}} < \frac{1}{(1-U)^2} = 3.041$$

which indicates a non-negligible deviation between the exact transducer gain G_T and the unilateral approximation G_{TU}. Therefore, the device cannot be accurately modeled as unilateral, and the matching networks must be designed using a bilateral approach. As demonstrated in [10], applying a rigorous bilateral design procedure is essential for GaN devices with non-zero reverse isolation to optimize the stability factor and guarantee precise conjugate impedance matching without unintended circuit degradation.

2.4.9. Gain circle and optimum load/source impedances

At 7.7 GHz, the maximum achievable gain after stabilization is approximately 18.24 dB. In this design, the target power gain is selected as

$$G_P = 18 \text{ dB}$$

The normalized gain parameter g_P is computed as

$$g_P = \frac{\mathrm{G_P}}{|\,\mathrm{S_{21}}\,|^2} = 6.454$$

The center C_L and radius R_L of the constant gain circle are calculated as

$$C_L = \frac{\mathrm{g_P}(\mathrm{S_{22}^*} - \Delta^*\mathrm{S_{11}})}{1 + \mathrm{g_P}(|\,\mathrm{S_{22}}\,|^2 - |\,\Delta\,|^2)} = 0.97\angle 54.7°$$

$$R_L = \frac{\sqrt{1 - 2\mathrm{K}\,|\,\mathrm{S_{12}S_{21}}\,|\,\mathrm{g_P} + |\,\mathrm{S_{12}S_{21}}\,|^2\,\mathrm{g_P^2}}}{|\,1 + \mathrm{g_P}(|\,\mathrm{S_{22}}\,|^2 - |\,\Delta\,|^2)\,|} = 0.103$$

A load impedance point on the $G_P = 18$ dBcircle is then selected as

$$Z_L = 15.84 + j92.44\Omega$$

Given Z_L, the input reflection coefficient Γ_{in} is computed by

$$\Gamma_{in} = S_{11} + \frac{S_{12}S_{21}\Gamma_L}{1 - S_{22}\Gamma_L}$$

and the optimum source reflection coefficient is chosen as $\Gamma_S = \Gamma_{in}^*$, resulting in

$$Z_S = 3.972 + j38.5\Omega$$

The gain circle, together with the selected Z_L and corresponding Z_S, is illustrated on the Smith chart in Fig. 8.

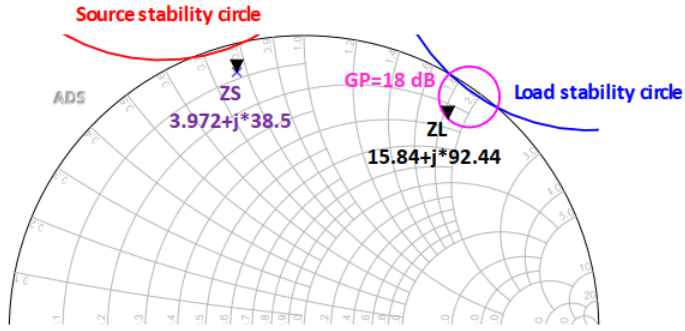

Fig. 8. Constant gain circle ($G_P = 18$ dB) and the selected Z_L and Z_S on the Smith chart.

Finally, simulation results using the selected Z_S and Z_L confirm compliance with the required performance targets, as shown in Fig. 9.

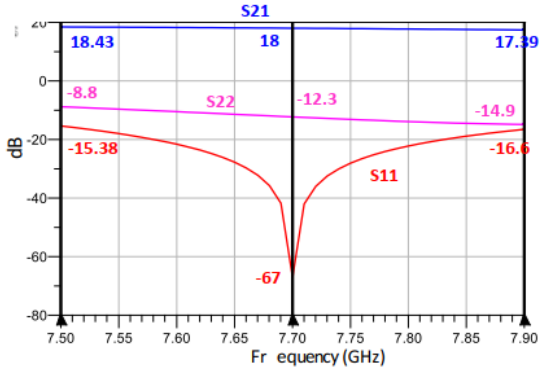

Fig. 9. Simulated S-parameters using the selected $Z_S$and Z_L.

3. BIAS NETWORK DESIGN

DC blocking capacitors are employed at both the input and output of the RF power amplifier to provide RF coupling between stages while isolating the DC bias voltages. In addition, these capacitors serve as RF grounding elements for the bias network. Therefore, the selected capacitors must exhibit low insertion loss at the operating frequency while effectively blocking DC components.

Several commercially available capacitors from the Murata library are evaluated, and the **GJM0335C1E1R7WB01** capacitor is selected due to its suitable frequency response at the target operating frequency of 7.7 GHz. The simulated frequency characteristic of the selected capacitor is shown in Fig. 10, demonstrating that it meets the RF coupling requirements with minimal insertion loss.

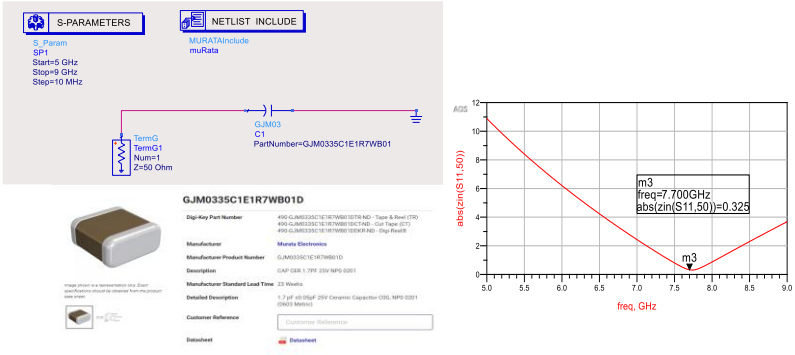

Fig. 10. Frequency response of the selected DC blocking capacitor.

The bias network is responsible for supplying the DC operating voltage to the GaN HEMT transistor while preventing RF signals from leaking into the DC power supply. To suppress the RF signal at the fundamental frequency, a quarter-wavelength (λ/4) transmission line with a short-circuited termination is employed in the bias network. At the operating frequency, this structure presents a high impedance to RF signals, thereby effectively isolating the RF path from the DC supply [4].

The schematic of the bias network and its simulated performance are shown in Fig. 11. The simulated insertion loss of the bias network is approximately S21 = −0.017 dB at 7.7 GHz, indicating negligible RF attenuation. The small loss observed is mainly attributed to conductor and dielectric losses in the transmission lines.

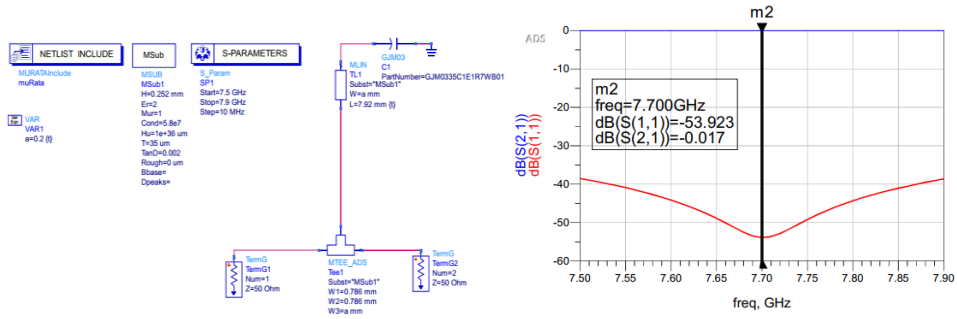

Fig. 11. Schematic and simulated performance of the bias network.

These results confirm that the proposed bias network provides effective DC feeding while maintaining excellent RF isolation, making it suitable for the designed RF power amplifier.

4. INPUT AND OUTPUT IMPEDANCE MATCHING NETWORK DESIGN

4.1. Input Matching Network Design

The input impedance matching network (IMN) is designed to efficiently transfer RF power from the signal source to the input of the GaN HEMT transistor. Its primary function is to transform the 50-Ω source impedance into the optimum source impedance previously determined through gain-circle analysis.

For the present design, a wideband matching approach is required to ensure that the performance specifications are satisfied over the frequency range from 7.5 GHz to 7.9 GHz. Based on the bilateral design procedure described in Section III, the optimum source impedance is selected as.

$$Z_S = 3.972 + j38.5\Omega$$

The input matching network is implemented using microstrip transmission-line sections. The detailed matching procedure is carried out on the Smith chart and is omitted here for brevity [1]. The resulting ideal matching network and its schematic-level implementation are shown in Fig. 12.

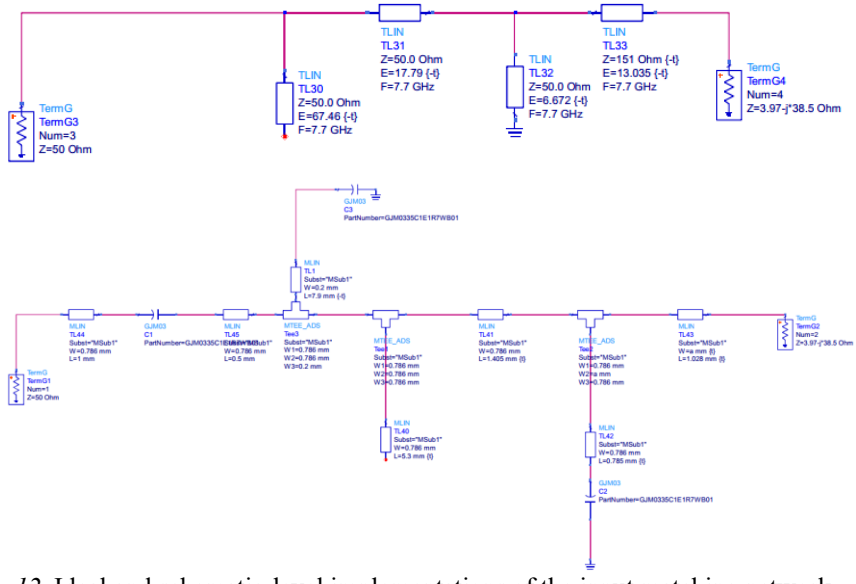

Fig. 12. Ideal and schematic-level implementations of the input matching network**.**

To evaluate the matching performance, the port connected to the transistor is terminated with the complex conjugate of the optimum source impedance Z_S^*. This setup allows the insertion loss S_{21} and input reflection coefficient S_{11} of the input matching network to be accurately assessed.

A strong correlation is observed between the simulated performances of the ideal and schematic-level input matching networks, validating the accuracy of the introduced design methodology. These comprehensive evaluation metrics are illustrated in Fig. 13

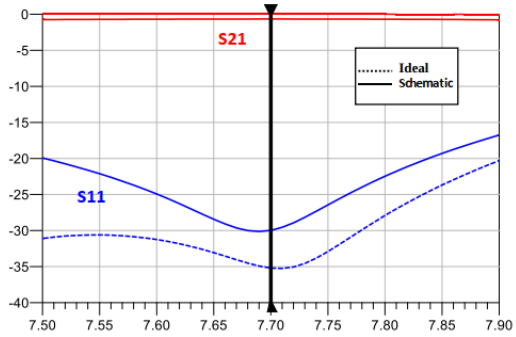

Fig. 13. Simulated performance of the input matching network at ideal and schematic levels.

4.2. Output Matching Network Design

The output matching network (OMN) of the RF power amplifier is designed to efficiently deliver the amplified RF power from the transistor output to the 50-Ω load. Based on the gain-circle analysis described earlier, the optimum load impedance is selected as

$$Z_L = 15.84 + j92.44\Omega$$

The output matching network is implemented using microstrip transmission-line sections to transform the optimum load impedance to the standard 50-Ω load. At the transistor side of the output matching network, the load is terminated with the complex conjugate impedance Z_L^* to accurately evaluate the matching performance.

The ideal and schematic-level implementations of the output matching network are shown in Fig. 14.

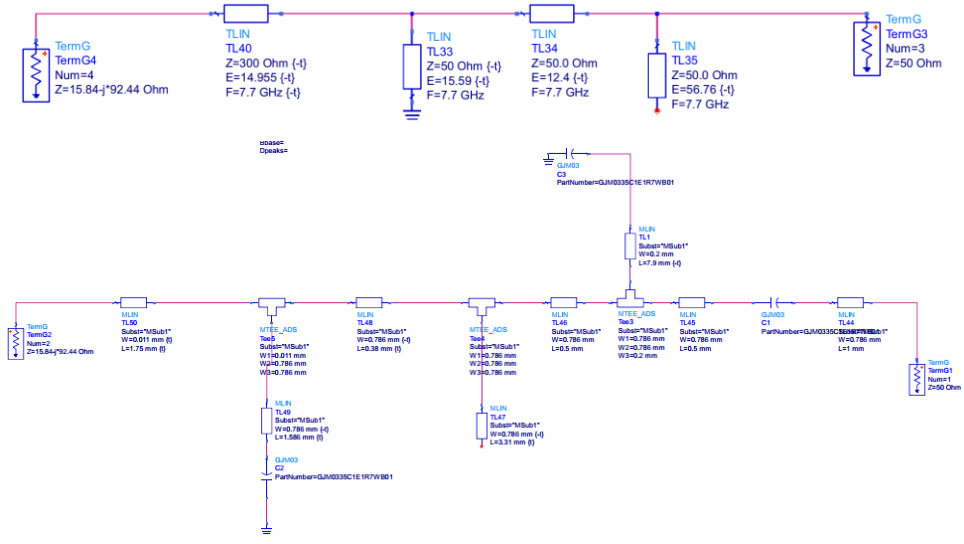

Fig. 14. Ideal and schematic-level implementations of the output matching network.

Simulation results demonstrate close agreement between the ideal and schematic-level designs, indicating that parasitic effects and transmission-line losses have minimal impact on the matching performance within the operating frequency range.

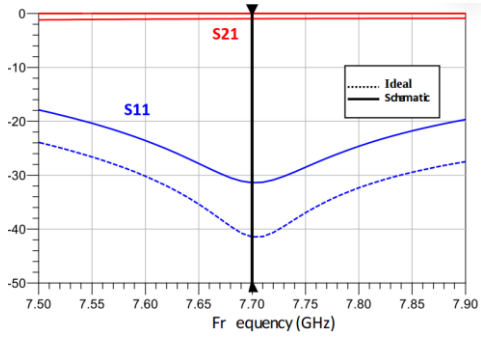

Fig. 15. Simulated performance of the output matching network at ideal and schematic levels.

Overall, the results confirm that the proposed output matching network is robust and that the schematic-level design closely approximates the ideal performance.

4.3. Full-Circuit Integration and Performance Verification

After designing the individual building blocks, including the bias network and the input and output matching networks, a full-circuit simulation is performed to evaluate the overall performance of the proposed RF power amplifier. The complete schematic of the amplifier is shown in Fig. 16.

In this simulation, all microstrip transmission lines are implemented at the schematic level, and the interconnections between the GaN HEMT transistor, the stabilization network, and the bias components are fully taken into account. This approach allows parasitic effects and transmission-line losses to be accurately reflected in the simulation results.

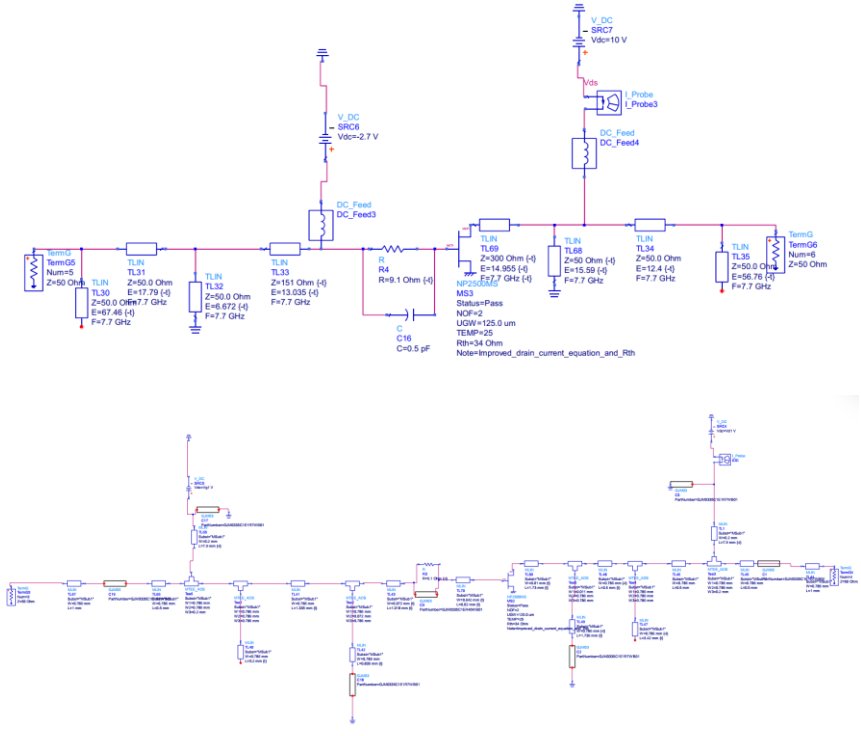

Fig. 16. Complete schematic of the proposed RF power amplifier.

4.4. Overall S-Parameter Performance

The simulated S-parameters of the complete RF power amplifier at both the ideal and schematic levels are presented in Fig. 17. Good agreement between the two levels is observed across the entire operating frequency range from 7.5 GHz to 7.9 GHz, corresponding to a fractional bandwidth of approximately 5.2%.

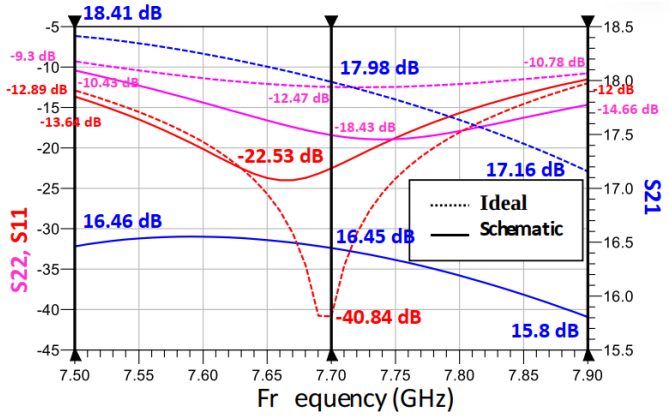

Fig. 17. Simulated S-parameters of the complete RF power amplifier at ideal and schematic levels.

At the schematic level, the forward gain S_{21}remains higher than 15.8 dB, while the input and output reflection coefficients satisfy $S_{11} < -12\text{dB}$ and $S_{22} < -9.3\text{dB}$ across the operating band. These results indicate that the proposed design meets all the specified S-parameter requirements.

The slight discrepancies between the ideal and schematic results can be attributed to dielectric and conductor losses in the substrate as well as parasitic effects introduced by lumped components such as capacitors and resistors. Nevertheless, the strong correlation between the two simulation levels confirms the accuracy and robustness of the proposed design methodology.

5. SIMULATION RESULTS AND DISCUSSION

5.1. S-Parameter Performance

The S-parameters of the proposed RF power amplifier are evaluated at the schematic level to verify compliance with the design specifications. The simulated results are presented in Fig. 18.

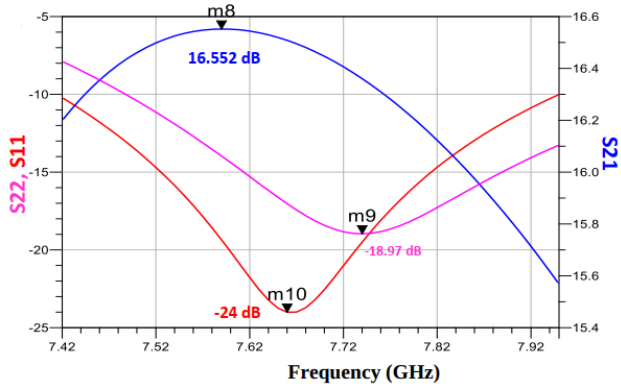

Fig. 18. Simulated S-parameters of the proposed RF power amplifier

The amplifier satisfies the required performance over the frequency range from 7.42 GHz to 7.95 GHz, corresponding to a fractional bandwidth of 6.9%. Within this band, the input reflection coefficient S_{11} remains below −10 dB, while the output reflection coefficient S_{22}remains below −7.88 dB.

At the center frequency of 7.66 GHz, the minimum value of S_{11} reaches −24 dB, and the minimum value of S_{22}reaches −18.97 dB at 7.74 GHz. The maximum forward gain $S_{21}$is 16.55 dB at 7.59 GHz. These results confirm excellent input/output matching and sufficient gain over the operating bandwidth.

5.2. Output Power and DC Power Consumption

According to the design specifications, the output power of the RF power amplifier must exceed 10 dBm over the operating band, while the DC power consumption must remain below 0.3 W. To evaluate these requirements, the output power and DC power consumption are analyzed as functions of the input power at the center frequency of 7.7 GHz, as shown in Fig. 19.

At 7.7 GHz, the amplifier achieves a maximum output power of 17.59 dBm while maintaining DC power consumption below 0.3 W. When the output power is set to 10 dBm, the corresponding DC power consumption is approximately 0.162 W. Based on these results, the input power is selected as $P_{in} = -2.2$ dBm for broadband evaluation.

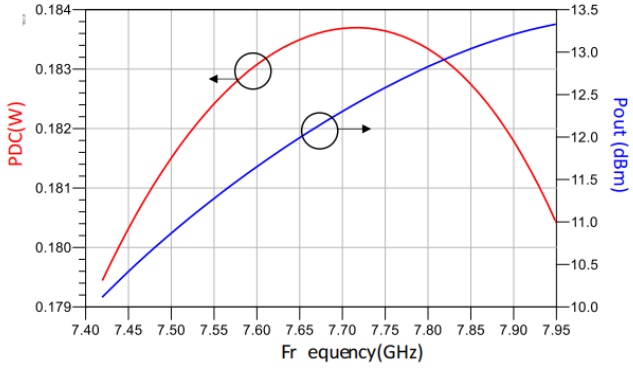

Fig. 19. Output power and DC power consumption versus input power at 7.7 GHz.

The frequency dependence of the output power and DC power consumption for $P_{in} = -2.2$dBm is shown in Fig. 20.

Over the frequency range from 7.42 GHz to 7.95 GHz, the output power remains above 10 dBm, while the DC power consumption remains below 0.184 W, which is significantly lower than the specified limit.

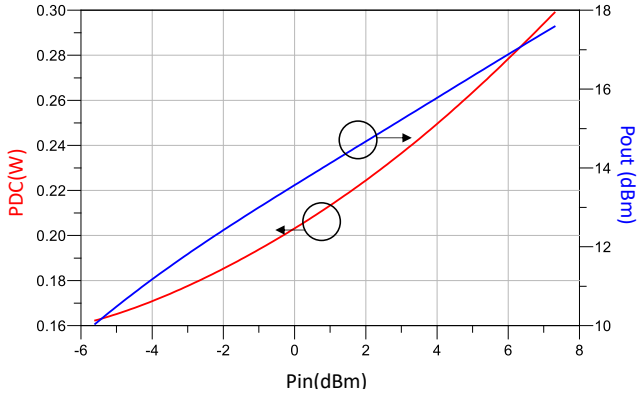

Fig. 20. Frequency characteristics of output power and DC power consumption.

5.3. Performance Summary

A comparison between the design requirements and the achieved simulation results is summarized in Table 4. It is evident that all specified performance criteria are fully satisfied.

Table 4. Comparison between design specifications and simulation results

Parameter	Specification	Simulated Result	Evaluation
S11 (dB)	≤ -10	-22.53	Satisfied
S22 (dB)	≤ -5	-18.429	Satisfied
P_{out} (dBm)	≥ 10	17.59	Satisfied
P_{DC} (W)	≤ 0.3	0.184	Satisfied
Bandwidth (%)	≥ 5	6.9	Satisfied

6. CONCLUSION

A 7.7-GHz RF power amplifier based on a GaN HEMT transistor implemented on a Rogers 5880LZ substrate has been successfully designed and simulated. The proposed amplifier achieves high gain, wide bandwidth, and unconditional stability while maintaining low DC power consumption. Simulation results confirm that all specified performance requirements are satisfied, including reflection coefficients, output power, and DC power consumption. Due to its favorable performance characteristics, the proposed design is well suited for applications in C-band microwave communication and radar systems.

REFERENCES

[1] D. M. Pozar, *Microwave Engineering*, 4th ed. Hoboken, NJ, USA: Wiley, 2012, doi: https://doi.org/10.1109/9780470631553

[2] S. C. Cripps, *RF Power Amplifiers for Wireless Communications*, 2nd ed.Norwood, MA, USA: Artech House, 2006. [Online]. Available: https://www.semanticscholar.org/paper/RF-Power-Amplifiers-for-Wireless-Communications-Cripps/dd3027bca402778da50334812674251db09cf931

[3] U. K. Mishra *et al*., "GaN-based RF power devices and amplifiers," *Proc. IEEE*, vol. 96, no. 2, pp. 287-305, Feb. 2008, doi: https://doi.org/10.1109/JPROC.2007.911060

[4] K. C. Gupta *et al., Microstrip Lines and Slotlines*, 2nd ed Norwood, MA, USA: Artech House, 1996, doi: https://doi.org/10.1109/LMWC.2021.3068593

[5] Rogers Corporation, "RO5880 and RO5880LZ High Frequency Laminates," Datasheet, 2020 . [Online]. Available: https://www.rogerscorp.com

[6] Y. Yang *et al.,* "A 7-9 GHz GaN HEMT power amplifier for C-band radar applications," *IEEE Microw. Wireless Compon. Lett.*, 2021, doi: https://doi.org/10.1109/LMWC.2021.3068593

[7] H. Wang *et al.,* "High-efficiency GaN HEMT power amplifier for microwave communication systems," *IEEE Trans. Microw. Theory Tech.*, 2020, doi: https://doi.org/10.1109/TMTT.2020.2985632

[8] J. J. Moreno, R. C. Callado, and M. S. Burgos, "High-Linearity and High-Efficiency Class-AB GaN HEMT Power Amplifiers with Compact Stabilization Networks for C-Band Applications," *IEEE Trans. Microw. Theory Tech.*, vol. 69, no. 5, pp. 2541–2553, May 2021, doi: https://doi.org/10.1109/TMTT.2021.3060676

[9] S. K. Dhar, K. M. Rahman, and M. A. S. Karal, "Design of a Wideband High-Gain GaN HEMT Power Amplifier on Low-Loss Rogers Substrate for Radar Communication Systems," *Int. J. Microw. Wireless Technol.*, vol. 14, no. 3, pp. 312–321, Apr. 2022, doi: https://doi.org/10.1017/S175907872100056X

[10] A. N. Carter and B. L. Smith, "Bilateral Matching Techniques and Stability Factor Optimization for Microwave GaN Power Amplifiers," *IEEE Microw. Wireless Compon. Lett.*, vol. 33, no. 8, pp. 985–988, Aug. 2023, doi: https://doi.org/10.1109/LMWC.2023.3283641